Quantum State Transfer in Ladder Systems with Cross-Correlated Disorder

M. S. S. Junior[a], G. M. A. Almeida[a], F. A. B. F. de Moura[a,*]

[a]Instituto de Física, Universidade Federal de Alagoas, 57072-900, Maceió, Alagoas, Brazil

Abstract

We explore a disordered ladder system as a potential platform for the transmission of a single qubit. The quantum channel consists of two coupled one-dimensional chains, with homogeneous intra- and interchain hoppings. We introduce diagonal cross-correlated disorder into the ladder by assigning opposite binary distributions across each leg. By adding two sites, one at each end of the ladder, we explore the conditions under which high-fidelity quantum state transfer can occur. A finite-size analysis shows that the cross-correlation is capable of maintaining good transfer fidelities even amid the presence of moderate disorder. Our findings contribute to the design of quasi-1D quantum channels prone to static parameter fluctuations for quantum communication devices.

1. Introduction

Achieving high-fidelity quantum state transfer (QST) and entanglement distribution are crucial goals for the development of quantum networks [1, 2]. Along this line of research, the transmission of an arbitrary qubit between distant parts of lattice systems has been widely studied since Bose's proposal [3] of harnessing the natural time evolution of spin chains for coherent excitation transport. Since then, numerous tight-binding models have been proposed, with distinct capabilities. Perfect QST, for instance, can be achieved upon judicious tuning of all the couplings across a one-dimensional chain [4, 5]. Another class of configuration, which delivers nearly-unit QST fidelities, employs optimized couplings only at the ends of the chain [6, 7]. At the weak-coupling limit [8], the dynamics effectively takes place on two-level or three-level [9] subspaces depending on the resonance conditions between the end sites and the channel. This configuration is particularly robust to static disorder in the parameters of the Hamiltonian [10, 11]. We also mention approaches based on the local application of strong magnetic fields [12], tailored inputs [13, 14], topological edge states [15, 16], flat bands [17], and others (reviews on the subject can be found in Refs. [18, 19, 20]). Various studies have also addressed the effects of noise in those protocols, including static parameter fluctuations [21, 22, 23, 24, 25, 26, 10, 27, 28, 29, 30, 31, 32, 33, 34, 35] and environmental decoherence [36, 37, 38]. In reality, achieving high-fidelity QST is challenging, as it requires systems that not only maintain coherence but also scale efficiently. Finding the right balance between size, transfer time, and fidelity has driven innovative research in QST across those engineering schemes.

Prototype QST Hamiltonians based on spin-1/2 chains have predominantly been one-dimensional. The relatively simple geometry, combined with the natural connectivity and inherent quantum correlations offered by spin chains, makes them promising platforms for exploring fundamental aspects of quantum transport. However, there remains much to explore if we allow ourselves to look beyond one-dimensional systems [17]. In this sense, ladder models have been a compelling framework for studying quantum transport phenomena [39, 40, 41, 42]. They provide an intermediate level of complexity that bridges the gap between linear chains and two-dimensional systems. A simple ladder system is composed of two coupled one-dimensional chains, enabling us to explore the rich dynamics arising from the interplay between intra- and interchain

---
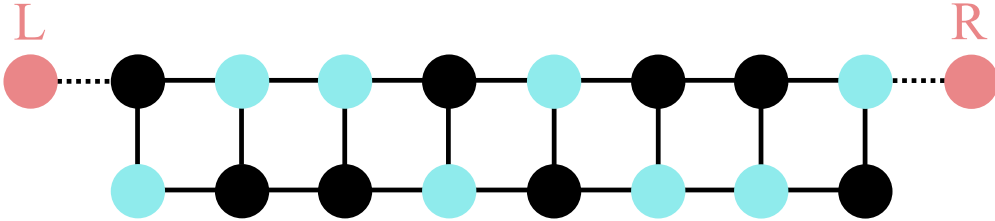
Figure 1: Schematic representation of the ladder model with $K = 8$. Solid edges correspond to the coupling strength J and the dotted ones at both ends of the upper leg denotes g, which couples the left (L) and right (R) communicating sites to the channel. Both are assigned a tunable local energy E_0. Dark and bright colors filling the nodes of the ladder indicate the binary distribution of the on-site disorder $\pm W$. The cross correlation is set by defining the on-site energies of one leg with the opposite sign with respect to the other.

interactions. For example, two-leg models can display metal-insulator transition with well defined mobility edges [43]. Certain correlations rotted on local constant proportions between the on-site potentials and interchain coupling strengths can also yield a band of delocalized states that coexists with strongly localized ones [44, 45]. In Ref. [40], a ladder spin-1/2 chain with such a correlated disorder was investigated in an entanglement transfer protocol. Notably, it was shown that increasing the disorder strength led to a higher transfer fidelity, which was measured by the concurrence. Furthermore, the involved transport properties of DNA molecules are often modeled by two-leg ladders with cross correlations in the potentials [46, 47].

Inspired by this, we investigate the effect of diagonal cross-correlated disorder on quantum state transfer in ladder systems. The communicating sites are weakly coupled to the ladder as shown in Fig. 1, a configuration proposed in Ref. [39]. In this work, however, we introduce the disorder by assigning a binary series to the on-site energies to one leg, with the other leg taking the opposite values. We will see that this type of correlation positively impacts the dynamics of the system in the context of QST due to the weakening of localization within certain energy ranges. From another point of view, the figure of merit of the QST protocol can also be used to measure the localization properties of the disordered ladder.

2. Model

Let us consider an isotropic XY (or, simply, XX) spin$-1/2$ chain expressed in terms of non-interacting spinless fermions (Jordan-Wigner transformation). The topology of the channel under consideration consists of two parallel chains, referred to as the upper and lower legs, each of length K. Both intra- and interchain couplings are given by J and form a ladder-like structure. At the upper leg, two extra sites, namely L and R are weakly coupled to it via $g \ll J$ [8, 39], hence the total number of sites is $N = 2K + 2$. The configuration is displayed in Fig. 1. (For all practical purposes, our findings would not differ quantitatively if, for example, site R were coupled to the lower leg.) The Hamiltonian reads

$$H = \sum_{i=1}^{K-1} J \left(u_i^\dagger u_{i+1} + d_i^\dagger d_{i+1} + \text{h.c.} \right) + \sum_{i=1}^{K} J \left(u_i^\dagger d_i + \text{h.c.} \right)$$

$$+ g(u_L^\dagger u_1 + u_R^\dagger u_K + \text{h.c.}) + \sum_{i=1}^{K} \epsilon_i \left(u_i^\dagger u_i - d_i^\dagger d_i \right) + E_0 \left(u_L^\dagger u_L + u_R^\dagger u_R \right), \qquad (1)$$

where $u_i^\dagger$ and $d_i^\dagger$ are fermionic creation operators at site i for the upper and lower legs, respectively. The local energy of the external sites is given by E_0, whereas those in the ladder are set by ϵ_i, to which we assign two possible values: $+W$ or $-W$, with equal probability, where W is a tunable parameter that controls the intensity of the disorder, which can be adjusted to explore different disorder regimes within the system. The cross correlation is already imposed by the term $\sum_{i=1}^{K} \epsilon_i \left(u_i^\dagger u_i - d_i^\dagger d_i \right)$ in Eq. (1) due to the opposite signs. It means that when a site in the upper leg is assigned the energy $+W$, the corresponding site in the other
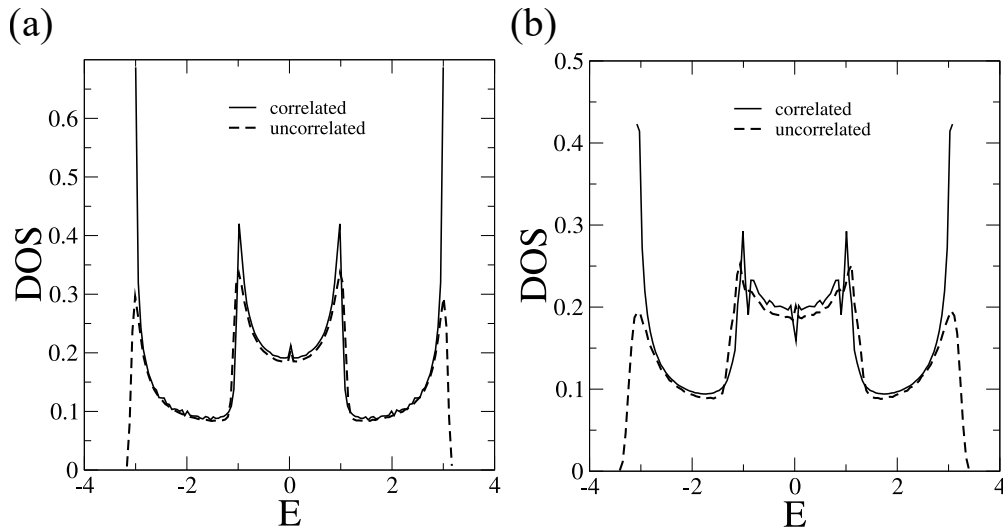
Figure 2: Normalized density of states (DOS) versus eigenenergies E of the ladder alone for the disorder strengths (a) $W = 0.25$ and (b) $W = 0.5$ comparing the correlated (solid curves) and uncorrelated (dotted curves) cases. The size of the ladder is $K = 2000$ and shown is the averaged DOS over 500 realizations of the disorder.

leg will be assigned the energy $-W$, and vice versa. The intra- and interchain couplings J will remain fixed throughout our discussion and thus we set $J \equiv 1$ as the standard energy unit.

The standard protocol for transmitting a single qubit in a XX spin$-1/2$ chain goes as follows (see [3, 19] for details). The whole system is initialized in the ferromagnetic ground state (all spins down) $|\text{ground}\rangle = |\downarrow\rangle_L |\Downarrow\rangle_{\text{ladder}} |\downarrow\rangle_R$. Then, the sender prepares its spin located in L in an arbitrary superposition of the form $|\psi\rangle_L = \alpha|\downarrow\rangle_L + \beta|\uparrow\rangle_L$ (α and β being complex amplitudes) such that the full input state reads $|\psi\rangle_L |\Downarrow\rangle_{\text{ladder}} |\downarrow\rangle_R$. The goal is to recover the input state at the receiver's site (R) at a prescribed time. Given the system Hamiltonian preserves the total number of excitations, we only need to keep track of the dynamics occurring in the single-excitation subspace. Indeed, a proper figure of merit of the QST protocol can be cast as a monotonic function of the transition amplitude $f_R(t) = \langle\text{ground}|u_R U(t) u_L^\dagger|\text{ground}\rangle$, where $U(t) = e^{-iHt}$ ($\hbar \equiv 1$) is the quantum time evolution operator. The so-called averaged fidelity (averaged over the whole Bloch sphere pertaining to the input state) reads [3]

$$F(t) = \frac{1}{2} + \frac{|f_R(t)|}{3} + \frac{|f_R(t)|^2}{6}. \qquad (2)$$

We emphasize that this quantity ranges from $F = 1/2$ to $F = 1$ (indicating perfect transfer). The threshold for the classical transmission of a quantum state is $F = 2/3$; thus a fidelity above this level justifies the functionality of the quantum channel.

The mechanism behind weakly-coupled QST schemes is the occurrence of Rabi oscillations involving the sites L and R. These are mediated by the channel modes [8, 9, 48], with the degree of population transfer depending on their localization properties [11]. If the energy of the weakly-coupled parties, E_0, meets a spectral region dominated by delocalized states, then greater is the capability of the channel to mediate the transfer, and even generate entanglement [11, 33]. The typical timescale of the effective Rabi dynamics is $\propto g^{-2}$ [8, 48]. Here, the minimum value of g we will consider is of the order of 10^{-2}. Considering that we are dealing with disordered samples, the overall performance of the protocol will be the assessed by the maximum fidelity $F_{\max}$ obtained over a time window $t \in [0, \tau]$, with $\tau \sim 10^5$, which ensures that the system has evolved long enough in the sense of transmitting the excitation from one end to the other.
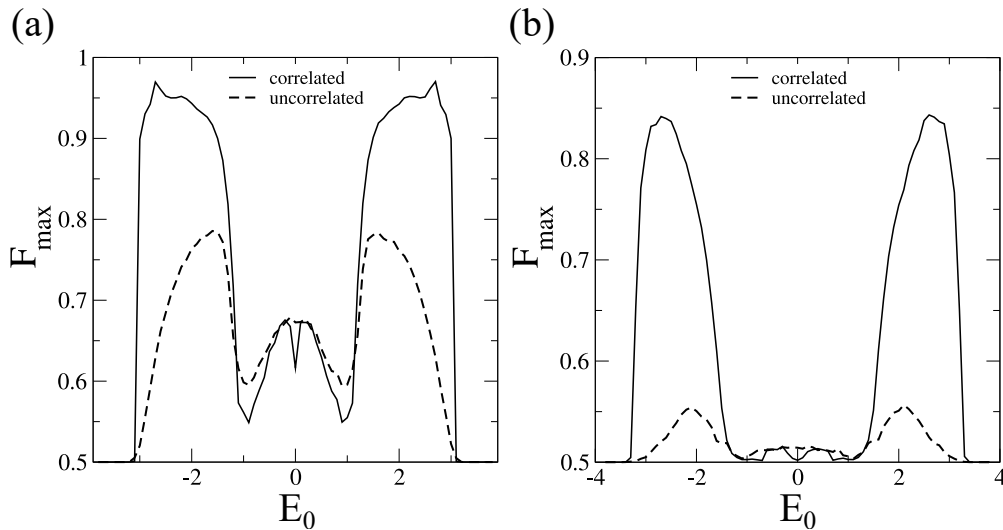
Figure 3: F_{max} as a function of the local energy E_0 of the communicating sites for disorder strengths (a) $W = 0.5$ and (b) $W = 1$. The weak coupling is fixed to $g = 0.025$, $N = 102$, and F_{max} is averaged over 1000 independent realizations of the disorder. Two transfer windows are observed around $E_0 \approx \pm 2.5$. These regions indicate the presence of delocalized modes within the channel.

3. Results

Our results are presented below. We would like stress that the computational approach we use to evaluate the quantum time evolution operator relies solely on the exact diagonalization of the Hamiltonian [Eq. (1)] in the single-excitation subspace. This method guarantees the accurate temporal evolution of the wave packet over long times without any degradation of the wave function's norm. The time evolution is computed in discrete time steps of size Δt. In our analysis, we explored a range of those, from relatively small values ($\Delta t < 1$) to larger ones ($\Delta t \approx 200$). Given the typical timescale of the Rabi dynamics that governs the QST, the obtained maximum fidelities (averaged over an ensemble of disorder realizations) remained consistent both qualitatively and quantitatively across that range. Consequently, most of our simulations were performed using $\Delta t \approx 200$ to optimize computational efficiency without compromising accuracy.

Before presenting the results for the QST itself, however, let us first have a rapid look into the spectral properties of the ladder channel (without sites L and R). In Fig. 2 we show the density of states (DOS) versus the channel's eigenenergies E for two different disorder strengths, $W = 0.25$ and $W = 0.5$. The DOS was obtained by building a histogram of the eigenvalues of the Hamiltonian, which were computed through exact diagonalization. The eigenvalues were grouped into bins of fixed width, and their count within each bin was divided by both the total number of modes and the bin width. This procedure ensures that the DOS is normalized, such that the integral of the DOS over the entire energy range equals one, allowing for a proper probabilistic interpretation of the energy distribution. In the figure we compare these results with those obtained from a similar model where the disorder is implemented by uncorrelated binary distributions along each leg. The results show that the structure of the allowed energy bands remains qualitatively unchanged. This suggests that, apart from the weakening of the expected singularities at the band edges, the disorder does not significantly alter the overall distribution of the energy spectrum in the model. Yet, we are about to see that the correlation is responsible for improving the QST quality significantly.

Now, in Fig. 3 we present the ensemble-averaged F_{max} as a function of tuning energy of the outermost sites L and R, E_0, for two disorder strengths, $W = 0.5$ and $W = 1$. In the correlated case, both panels reveal the existence of two distinct transfer windows, centered around $E \approx 2.5$. These windows have an approximate width of $\Delta E \approx 0.2$, which appears to decrease as the disorder strength W increases. Those transfer windows correspond to regions where the fidelity of the QST is maximized (greater than the classical threshold of 2/3), indicating that delocalized states are present in the range [11]. In contrast, outside these

4
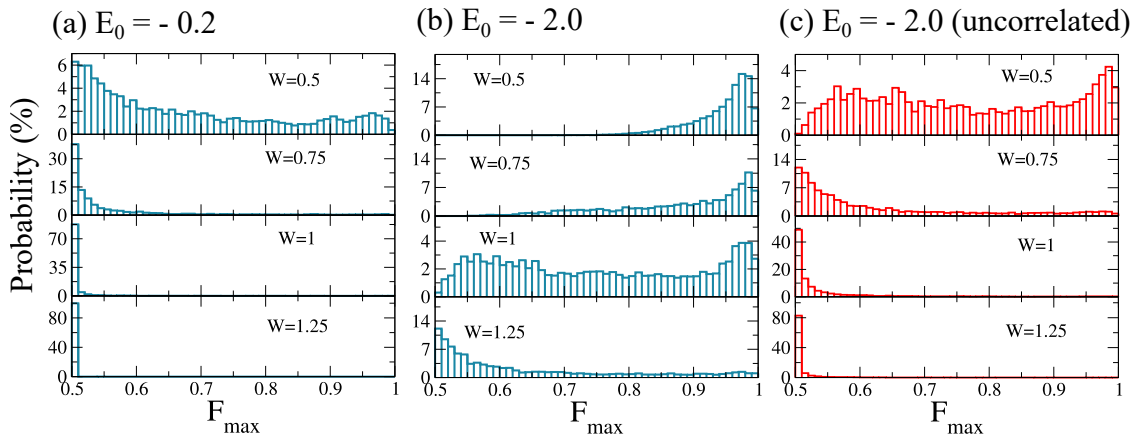
Figure 4: Probability distribution of F_{max} for different disorder strengths W and local energies: (a) $E_0 = -0.2$, (b) $E_0 = -2.0$, and (c) $E_0 = -2.0$ but for the uncorrelated case. Fixed system parameters are $N = 102$ and $g = 0.025$. Each histogram is generated 1000 independent disordered samples. A comparison between panels (b) and (c) highlights the importance of disorder correlations for enabling a high-fidelity QST protocol.

windows, particularly at the extremes of the band and near the center of the band, the fidelity dramatically drops. This is clear signature that the underlying two-level (Rabi) dynamics between sites L and R is highly out of resonance. For comparison, in Fig. 3 we include the corresponding results for the uncorrelated case We observe that the fidelity is significantly lower than in the case with cross-correlated disorder, underscoring the important role of the disorder correlations in enhancing QST quality.

To further address the importance of picking the right tuning energy E_0, Fig. 4 depicts the probability distribution of F_{max} for two tuning energies, $E_0 = -0.2$ and $E_0 = -2.0$, each standing for distinct transfer qualities. Figures 4(a) and 4(b) display the results for the correlated case. For $E_0 = -0.2$ [4(a)], we see that even in the weak disorder regime ($W = 0.5$), the distribution bends toward $F_{max} = 1/2$. As W increases, this trend becomes even more pronounced, ultimately suppressing the QST. These findings imply that the channel modes are strongly localized at energies close to E_0, despite the presence of correlations in the disorder. For $E_0 = -2.0$ [4(b)], on the other hand, a strikingly different behavior is observed. For disorder strengths up to intermediate values, $W \leq 1$, chances are high that fidelities above 0.95 are obtained. Comparing those histograms with the corresponding uncorrelated case [4(c)], with the same parameters, we once again highlight the role of the cross correlations in boosting the QST performance.

Now, we explore the role of the weak coupling parameter g. As already mentioned, in the perturbative limit the QST timescale scales as g^{-2}. Hence, there must be a tradeoff between QST speed and fidelity [8, 48]. In Fig. 5(a), F_{max} is evaluated against g for $E_0 = 2.5$, which is a proper tuning energy for the protocol (cf. Fig. 3). We note that F_{max} decreases almost linearly with g, up to $g = 0.225$ (starting from 0.01), and yet the fidelities are maintained above the classical threshold of 2/3 for all values of W considered. Overall, the decrease in QST quality in this case should be understood not in terms of the localization properties of the channel modes around $E \approx E_0$. Rather, as g increases the effective two-level dynamics ceases to exist [9], with the single excitation states associated to sites L and R becoming more mixed with the ladder modes. The dynamics thus becomes more dispersive while the transport properties of the ladder alone remain the same, as the parameters of the bulk have not changed. While out of the scope of the present work, it is worth mentioning that in homogeneous one-dimensional models, a kind of ballistic regime can be achieved at optimal (not perturbative) values of g, yielding a fast QST with high fidelities [7]. Therefore, models with tunable couplings at the boundaries offer a versatile plataform for designing quantum communication schemes.

Another parameter that affects the QST performance is the system size N. Figure 5(b) displays F_{max} as N grows. In this case, more ladder modes fill in the region surrounding $E \approx E_0$. As a consequence, if the perturbative regime $g \ll J$ is to be maintained, g must be decreased even further. In Ref. [8], it is

5

(a)   (b)
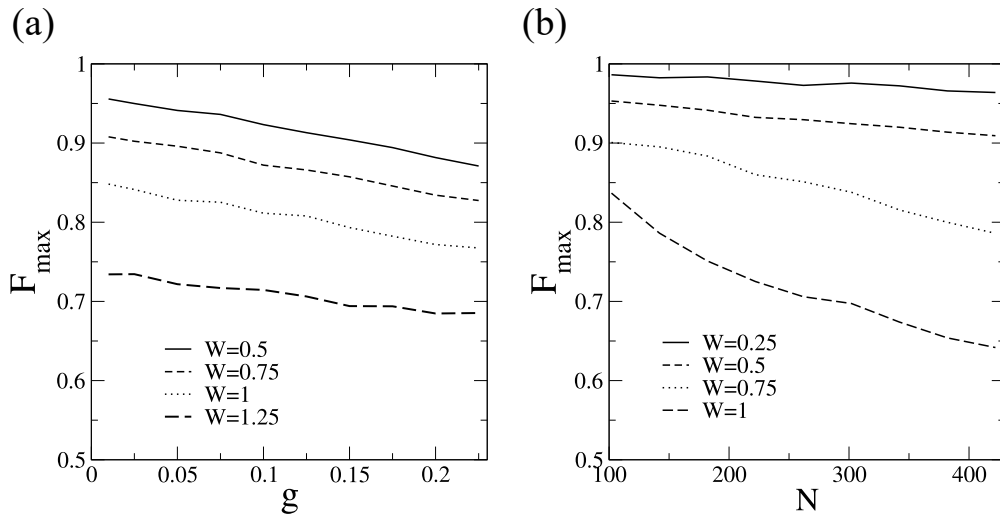
Figure 5: (a) $F_{\max}$ as a function of g for $E_0 = 2.5$, $N = 102$, and various disorder strengths W. (b) $F_{\max}$ as a function of system size N (from $N = 102$ to $N = 442$) for fixed $g = 0.025$ and $E_0 = 2.5$. All the curves represent $F_{\max}$ averaged over 1000 independent realizations of the disorder.
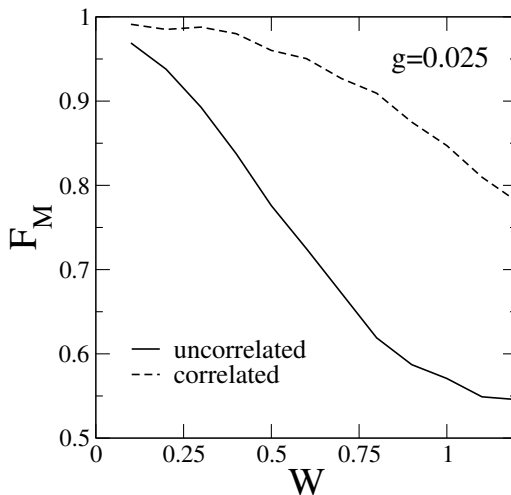
Figure 6: Figure 6 shows F_M as a function of W, where F_M represents the maximum average fidelity within the band of allowed states. In the correlated disorder case, F_M remains above 0.9 for disorder ($W \lesssim 0.7$) and decreases gradually in the intermediate-to-strong disorder regime . In contrast, in the uncorrelated case, F_M exceeds 0.9 only for very weak disorder ($W \lesssim 0.2$) and decays sharply for $W > 0.2$, reaching values close to 0.5. This highlights the role of cross-correlations in maintaining high fidelity even in the intermediate disorder regime.

reported that $g \ll 1/\sqrt{N}$ so as to keep the fidelity close to unit in homogeneous chains. Even though our system possesses a distinct geometry and is embedded with correlated disorder, the condition holds. We point out that a distinct behavior is observed when considering topological lattices, such as those providing topologically protected edges states separated by a gap, which does not close upon increasing N [15]. We also note in Fig. 5(b) that the fidelity decays more rapidly with N as W becomes higher. This indicates that, in addition to the influence of an effectively larger g explained above, the localization strength of the channel modes becomes more pronounced channel modes builds up more robustly as finite-size effects are minimized.

Before finishing our work, we will discuss some calculations presented in Figure 6, which shows F_M as

a function of W. The quantity F_M represents the maximum value of the average fidelity within the band of allowed states. Specifically, we compute the average fidelity within the band (considering initial state energies E_0 between -3.5 and 3.5) and identify its highest value within this range, which we denote as F_M. We then plot F_M as a function of W, considering both correlated and uncorrelated disorder cases. In the correlated case, for weak disorder ($W = 0.1$ to approximately $W = 0.7$), F_M remains close to 1 (above 0.9). For $W > 0.7$, the maximum fidelity in the band (F_M) decreases further, reaching values close to 0.8 when the disorder strength becomes comparable to the mean hopping term (i.e., W around 1 or slightly higher). This corresponds to an intermediate-to-strong disorder regime. On the other hand, in the uncorrelated case, F_M exceeds 0.9 only in the very weak disorder regime ($W = 0.1$ or $W = 0.2$). For $W > 0.2$, F_M starts to decay much more sharply compared to the correlated case, eventually reaching values close to the minimum 0.5. This figure clearly demonstrates that cross-correlations can sustain fidelity close to 1 even in the intermediate disorder regime. In contrast, in the absence of correlations, the system becomes ineffective for quantum state transfer when the disorder reaches a level comparable to the hopping energy.

4. Conclusion

In this work, we investigated quantum state transfer (QST) in a disordered ladder system with cross-correlated on-site disorder. The channel topology consists of two parallel chains, referred to as the upper and lower legs, each of length K. Both intra- and interchain couplings are given by J, forming a ladder-like structure. In the upper leg, two additional sites, labeled L and R, are weakly coupled to the system via $g \ll J$, bringing the total number of sites to $N = 2K + 2$. The system is modeled as an isotropic XX spin-$\frac{1}{2}$ chain, which can be mapped onto a system of spinless fermions via the Jordan-Wigner transformation. We examined how disorder and coupling parameters influence the efficiency of state transmission within this framework. Our results indicate that cross-correlations within the channel play a crucial role in achieving high transfer fidelities, particularly by tuning the local energy E_0 of the communicating sites. Using exact diagonalization techniques, we analyzed the spectral properties of the ladder system and identified transfer windows where QST is feasible. Despite the tendency of disorder to induce localization, we found that the cross-correlated structure alters the spectral characteristics in a way that enables efficient transmission. Additionally, our computational analysis demonstrated that the obtained fidelities remain robust across a broad range of time step sizes, ensuring the reliability of our numerical simulations. Our findings provide deeper insight into how correlated disorder influences transport properties in quantum systems and could have practical implications for quantum communication in engineered spin chains. Future research could explore alternative disorder correlations, nonreciprocal configurations, or interaction effects to further refine the understanding of quantum transport in complex disordered systems.

5. Acknowledgments

References

[1] J. I. Cirac, P. Zoller, H. J. Kimble, H. Mabuchi, Quantum state transfer and entanglement distribution among distant nodes in a quantum network, Phys. Rev. Lett. 78 (1997) 3221.

[2] H. J. Kimble, The quantum internet, Nature 453 (2008) 1023.

[3] S. Bose, Quantum communication through an unmodulated spin chain, Phys. Rev. Lett. 91 (2003) 207901. doi:10.1103/PhysRevLett.91.207901.
URL http://link.aps.org/doi/10.1103/PhysRevLett.91.207901

[4] M. B. Plenio, J. Hartley, J. Eisert, Dynamics and manipulation of entanglement in coupled harmonic systems with many degrees of freedom, New Journal of Physics 6 (1) (2004) 36.
URL http://stacks.iop.org/1367-2630/6/i=1/a=036

[5] M. Christandl, N. Datta, A. Ekert, A. J. Landahl, Perfect state transfer in quantum spin networks, Phys. Rev. Lett. 92 (2004) 187902. doi:10.1103/PhysRevLett.92.187902.
URL http://link.aps.org/doi/10.1103/PhysRevLett.92.187902

[6] L. Banchi, T. J. G. Apollaro, A. Cuccoli, R. Vaia, P. Verrucchi, Optimal dynamics for quantum-state and entanglement transfer through homogeneous quantum systems, Phys. Rev. A 82 (2010) 052321. `doi:10.1103/PhysRevA.82.052321`.
URL `https://link.aps.org/doi/10.1103/PhysRevA.82.052321`

[7] T. J. G. Apollaro, L. Banchi, A. Cuccoli, R. Vaia, P. Verrucchi, 99%-fidelity ballistic quantum-state transfer through long uniform channels, Phys. Rev. A 85 (2012) 052319. `doi:10.1103/PhysRevA.85.052319`.
URL `http://link.aps.org/doi/10.1103/PhysRevA.85.052319`

[8] A. Wójcik, T. Łuczak, P. Kurzyński, A. Grudka, T. Gdala, M. Bednarska, Unmodulated spin chains as universal quantum wires, Phys. Rev. A 72 (2005) 034303. `doi:10.1103/PhysRevA.72.034303`.
URL `http://link.aps.org/doi/10.1103/PhysRevA.72.034303`

[9] A. Wójcik, T. Łuczak, P. Kurzyński, A. Grudka, T. Gdala, M. Bednarska, Multiuser quantum communication networks, Phys. Rev. A 75 (2007) 022330. `doi:10.1103/PhysRevA.75.022330`.
URL `https://link.aps.org/doi/10.1103/PhysRevA.75.022330`

[10] A. Zwick, G. A. Álvarez, J. Stolze, O. Osenda, Quantum state transfer in disordered spin chains: how much engineering is reasonable?, Quant. Inf. Comp. 15 (2015) 852.

[11] G. M. A. Almeida, F. A. B. F. de Moura, M. L. Lyra, High-fidelity state transfer through long-range correlated disordered quantum channels, Phys. Lett. A 382 (2018) 1335.

[12] S. Lorenzo, T. J. G. Apollaro, A. Sindona, F. Plastina, Quantum-state transfer via resonant tunneling through local-field-induced barriers, Phys. Rev. A 87 (2013) 042313. `doi:10.1103/PhysRevA.87.042313`.
URL `http://link.aps.org/doi/10.1103/PhysRevA.87.042313`

[13] D. Burgarth, S. Bose, Perfect quantum state transfer with randomly coupled quantum chains, New Journal of Physics 7 (2005) 135. `doi:10.1088/1367-2630/7/1/135`.

[14] H. L. Haselgrove, Optimal state encoding for quantum walks and quantum communication over spin systems, Phys. Rev. A 72 (2005) 062326. `doi:10.1103/PhysRevA.72.062326`.
URL `https://link.aps.org/doi/10.1103/PhysRevA.72.062326`

[15] G. M. A. Almeida, F. Ciccarello, T. J. G. Apollaro, A. M. C. Souza, Quantum-state transfer in staggered coupled-cavity arrays, Phys. Rev. A 93 (2016) 032310. `doi:10.1103/PhysRevA.93.032310`.
URL `https://link.aps.org/doi/10.1103/PhysRevA.93.032310`

[16] S. Longhi, G. L. Giorgi, R. Zambrini, Landau–zener topological quantum state transfer, Advanced Quantum Technologies 2 (3-4) (2019) 1800090. `arXiv:https://onlinelibrary.wiley.com/doi/pdf/10.1002/qute.201800090`, `doi:https://doi.org/10.1002/qute.201800090`.
URL `https://onlinelibrary.wiley.com/doi/abs/10.1002/qute.201800090`

[17] G. M. A. Almeida, R. F. Dutra, A. M. C. Souza, M. L. Lyra, F. A. B. F. de Moura, Flat-band quantum communication induced by disorder, Phys. Rev. A 108 (2023) 022407. `doi:10.1103/PhysRevA.108.022407`.
URL `https://link.aps.org/doi/10.1103/PhysRevA.108.022407`

[18] A. Kay, Perfect, efficient, state transfer and its application as a constructive tool, Int. J. Quantum Inform. 08 (2010) 641.

[19] T. J. G. Apollaro, S. Lorenzo, F. Plastina, Transport of quantum correlations across a spin chain, Int. J. Mod. Phys. B 27 (2013) 1345035.

[20] G. M. Nikolopoulos, I. Jex (Eds.), Quantum State Transfer and Network Engineering, Springer-Verlag, Berlin, 2014.

[21] G. De Chiara, D. Rossini, S. Montangero, R. Fazio, From perfect to fractal transmission in spin chains, Phys. Rev. A 72 (2005) 012323. `doi:10.1103/PhysRevA.72.012323`.
URL `https://link.aps.org/doi/10.1103/PhysRevA.72.012323`

[22] J. Fitzsimons, J. Twamley, Superballistic diffusion of entanglement in disordered spin chains, Phys. Rev. A 72 (2005) 050301. `doi:10.1103/PhysRevA.72.050301`.
URL `https://link.aps.org/doi/10.1103/PhysRevA.72.050301`

[23] D. I. Tsomokos, M. J. Hartmann, S. F. Huelga, M. B. Plenio, Entanglement dynamics in chains of qubits with noise and disorder, New Journal of Physics 9 (3) (2007) 79.
URL `http://stacks.iop.org/1367-2630/9/i=3/a=079`

[24] S. M. Giampaolo, F. Illuminati, Long-distance entanglement in many-body atomic and optical systems, New Journal of Physics 12 (2010) 025019.

[25] N. Y. Yao, L. Jiang, A. V. Gorshkov, Z.-X. Gong, A. Zhai, L.-M. Duan, M. D. Lukin, Robust quantum state transfer in random unpolarized spin chains, Phys. Rev. Lett. 106 (2011) 040505. `doi:10.1103/PhysRevLett.106.040505`.
URL `http://link.aps.org/doi/10.1103/PhysRevLett.106.040505`

[26] A. Zwick, G. A. Álvarez, J. Stolze, O. Osenda, Spin chains for robust state transfer: Modified boundary couplings versus completely engineered chains, Phys. Rev. A 85 (2012) 012318. `doi:10.1103/PhysRevA.85.012318`.
URL `http://link.aps.org/doi/10.1103/PhysRevA.85.012318`

[27] M. Bruderer, K. Franke, S. Ragg, W. Belzig, D. Obreschkow, Exploiting boundary states of imperfect spin chains for high-fidelity state transfer, Phys. Rev. A 85 (2012) 022312. `doi:10.1103/PhysRevA.85.022312`.
URL `https://link.aps.org/doi/10.1103/PhysRevA.85.022312`

[28] S. Ashhab, Quantum state transfer in a disordered one-dimensional lattice, Phys. Rev. A 92 (2015) 062305. `doi:10.1103/PhysRevA.92.062305`.
URL `https://link.aps.org/doi/10.1103/PhysRevA.92.062305`

[29] A. Kay, Quantum error correction for state transfer in noisy spin chains, Phys. Rev. A 93 (2016) 042320. `doi:10.1103/PhysRevA.93.042320`.
URL `https://link.aps.org/doi/10.1103/PhysRevA.93.042320`

[30] M. P. Estarellas, I. D'Amico, T. P. Spiller, Robust quantum entanglement generation and generation-plus-storage protocols

with spin chains, Phys. Rev. A 95 (2017) 042335. `doi:10.1103/PhysRevA.95.042335`.
URL `https://link.aps.org/doi/10.1103/PhysRevA.95.042335`

[31] G. Almeida, C. Mendes, M. Lyra, F. de Moura, Localization properties and high-fidelity state transfer in hopping models with correlated disorder, Annals of Physics 398 (2018) 180–189. `doi:https://doi.org/10.1016/j.aop.2018.09.003`.
URL `https://www.sciencedirect.com/science/article/pii/S0003491618302422`

[32] P. Júnior, G. Almeida, M. Lyra, F. de Moura, Quantum communication through chains with diluted disorder, Physics Letters A 383 (16) (2019) 1845–1849. `doi:https://doi.org/10.1016/j.physleta.2019.03.010`.
URL `https://www.sciencedirect.com/science/article/pii/S0375960119302221`

[33] G. M. A. Almeida, F. A. B. F. de Moura, M. L. Lyra, Entanglement generation between distant parties via disordered spin chains, Quantum Information Processing 18 (2) (2019) 41. `doi:10.1007/s11128-018-2157-6`.
URL `https://doi.org/10.1007/s11128-018-2157-6`

[34] D. Messias, C. Mendes, G. Almeida, M. Lyra, F. de Moura, Rabi-like quantum communication in an aperiodic spin-1/2 chain, Journal of Magnetism and Magnetic Materials 505 (2020) 166730. `doi:https://doi.org/10.1016/j.jmmm.2020.166730`.
URL `https://www.sciencedirect.com/science/article/pii/S0304885319338958`

[35] Y. Ji, Z. Wu, R. Liu, Y. Li, F. Jin, H. Zhou, X. Peng, Inverse engineering for robust state transport along a spin chain via low-energy subspaces, New Journal of Physics 26 (1) (2024) 013041. `doi:10.1088/1367-2630/ad19fd`.
URL `https://dx.doi.org/10.1088/1367-2630/ad19fd`

[36] J.-M. Cai, Z.-W. Zhou, G.-C. Guo, Decoherence effects on the quantum spin channels, Phys. Rev. A 74 (2006) 022328. `doi:10.1103/PhysRevA.74.022328`.
URL `https://link.aps.org/doi/10.1103/PhysRevA.74.022328`

[37] W. Qin, C. Wang, X. Zhang, Protected quantum-state transfer in decoherence-free subspaces, Phys. Rev. A 91 (2015) 042303. `doi:10.1103/PhysRevA.91.042303`.
URL `https://link.aps.org/doi/10.1103/PhysRevA.91.042303`

[38] G. Mouloudakis, T. Ilias, P. Lambropoulos, Arbitrary-length xx spin chains boundary-driven by non-markovian environments, Phys. Rev. A 105 (2022) 012429. `doi:10.1103/PhysRevA.105.012429`.
URL `https://link.aps.org/doi/10.1103/PhysRevA.105.012429`

[39] Y. Li, T. Shi, B. Chen, Z. Song, C.-P. Sun, Quantum-state transmission via a spin ladder as a robust data bus, Phys. Rev. A 71 (2005) 022301. `doi:10.1103/PhysRevA.71.022301`.
URL `https://link.aps.org/doi/10.1103/PhysRevA.71.022301`

[40] G. M. Almeida, A. M. Souza, F. A. de Moura, M. L. Lyra, Robust entanglement transfer through a disordered qubit ladder, Physics Letters A 383 (27) (2019) 125847. `doi:https://doi.org/10.1016/j.physleta.2019.125847`.
URL `https://www.sciencedirect.com/science/article/pii/S0375960119306358`

[41] J. Zurita, C. E. Creffield, G. Platero, Fast quantum transfer mediated by topological domain walls, Quantum 7 (2023) 1043. `doi:10.22331/q-2023-06-22-1043`.
URL `https://doi.org/10.22331/q-2023-06-22-1043`

[42] M. Motamedifar, M. Abbasi, M. Golshani, A.-B. A. Mohamed, A. H. Homid, Which spin ladders are the most effective at transferring entanglements: two-legs or honeycombs!?, The European Physical Journal Plus 139 (1) (2024) 18. `doi:10.1140/epjp/s13360-023-04820-6`.
URL `https://doi.org/10.1140/epjp/s13360-023-04820-6`

[43] S. Sil, S. K. Maiti, A. Chakrabarti, Metal-insulator transition in an aperiodic ladder network: An exact result, Phys. Rev. Lett. 101 (2008) 076803. `doi:10.1103/PhysRevLett.101.076803`.
URL `https://link.aps.org/doi/10.1103/PhysRevLett.101.076803`

[44] S. Sil, S. K. Maiti, A. Chakrabarti, Ladder network as a mesoscopic switch: An exact result, Phys. Rev. B 78 (2008) 113103. `doi:10.1103/PhysRevB.78.113103`.
URL `https://link.aps.org/doi/10.1103/PhysRevB.78.113103`

[45] F. A. B. F. de Moura, R. A. Caetano, M. L. Lyra, Stationary, dynamical, and spectral electronic properties of a correlated random ladder model with coexisting extended and localized states, Phys. Rev. B 81 (2010) 125104. `doi:10.1103/PhysRevB.81.125104`.
URL `https://link.aps.org/doi/10.1103/PhysRevB.81.125104`

[46] R. A. Caetano, P. A. Schulz, Sequencing-independent delocalization in a dna-like double chain with base pairing, Phys. Rev. Lett. 95 (2005) 126601. `doi:10.1103/PhysRevLett.95.126601`.
URL `https://link.aps.org/doi/10.1103/PhysRevLett.95.126601`

[47] R. C. P. Carvalho, M. L. Lyra, F. A. B. F. de Moura, F. Domínguez-Adame, Localization on a two-channel model with cross-correlated disorder, Journal of Physics: Condensed Matter 23 (17) (2011) 175304. `doi:10.1088/0953-8984/23/17/175304`.
URL `https://dx.doi.org/10.1088/0953-8984/23/17/175304`

[48] G. M. A. Almeida, Interplay between speed and fidelity in off-resonant quantum-state-transfer protocols, Phys. Rev. A 98 (2018) 012334. `doi:10.1103/PhysRevA.98.012334`.
URL `https://link.aps.org/doi/10.1103/PhysRevA.98.012334`